

# Modeling and Simulation of Airflow Dynamics in a Dynamic Skip Fire Engine

2015-01-1717  
Published 04/14/2015

Li-Chun Chien, Matthew Younkings, and Mark Wilcutts

Tula Technology Inc.

**CITATION:** Chien, L., Younkings, M., and Wilcutts, M., "Modeling and Simulation of Airflow Dynamics in a Dynamic Skip Fire Engine," SAE Technical Paper 2015-01-1717, 2015, doi:10.4271/2015-01-1717.

Copyright © 2015 SAE International

## Abstract

Dynamic skip fire is a control method for internal combustion engines in which engine cylinders are selectively fired or skipped to meet driver torque demand. In this type of engine operation, fueling, and possibly intake and exhaust valves of each cylinder are actuated on an individual firing opportunity basis. The ability to operate each cylinder at or near its best thermal efficiency, and to achieve flexible control of acoustic and vibrational excitations has been described in previous publications.

Due to intermittent induction and exhaust events, air induction and torque production in a DSF engine can vary more than conventional engines on a cycle-to-cycle basis. This paper describes engine thermofluid modeling for this type of operation for purposes of air flow and torque prediction. Development of a one-dimensional model of medium complexity is described, along with solutions for practical issues encountered with the standard configuration of one-dimensional simulation packages such as GT-SUITE.

Airflow dynamic and thermodynamic simulation results for skip fire engine operation are presented and compared with experimental data under several different firing sequences. The dependence of air charge and net indicated mean effective pressure on skip fire sequence is illustrated.

Finally, a method of air estimation compensation is described via characterization of each induction event by skip history, both of the particular cylinder as well as previous cylinders in the firing order.

## Introduction

Cylinder deactivation is an established technology that assists in improving fuel economy in many throttled engine applications. A broad survey of such technology was discussed in [1]. Cylinder deactivation systems in current production switch to one or at most two reduced cylinder sets, such as eight to four cylinders or six to four to three [2, 3, 4].

Over the years, a number of skip-fire engine control arrangements have been proposed which do not simply switch back and forth to reduced cylinder sets. Förster et al [5] described use of a relatively large number of fixed cylinder fire-skip patterns but did not describe how the fixed patterns could be switched in order to effectively achieve smooth torque delivery in practice.

In contrast to these strategies, Tula Technology's Dynamic Skip Fire (DSF) considers activation or deactivation of each cylinder event independently, varying the density firings as driver demanded torque changes. Figure 1 shows the simple concept of using density of cylinder firings to produce a driver-demanded torque.

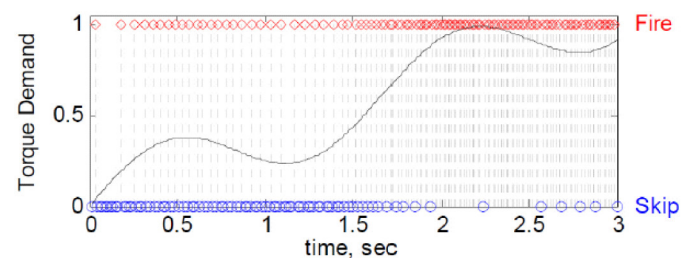


Figure 1. Dynamic Skip Fire concept achieves engine load control by varying cylinder firing density

With this system cycle average fuel economy has been demonstrated to improve by 14% to 21% [1]. An overview of the system, including fuel economy benefits, implementation, and noise, vibration and harshness (NVH) performance are described in [1]. An in-depth analysis of the root causes of NVH, proposed metrics, algorithmic and physical mitigation methods; and evaluation results are given in [6]. In contrast, this paper concerns the thermofluid modeling of a dynamic skip firing engine and does not discuss NVH, drivability, emissions, or durability.

In most conventional cylinder deactivation system applications such as [2, 3, 4] or camless engines [7], engine load is mainly controlled by throttle or valve timing within a small number of reduced cylinder sets. Each reduced cylinder set defines an air estimation mode, in which the air estimation algorithm does not require significant

modification. The modification may simply consist of a calibration table switch from one mode to the other, without change to the overall estimation scheme [8][9]. In DSF operation the number and sequence of firing cylinders is a continuously varying quantity. This flexibility adds a potential challenge to conventional air estimation schemes.

The present study uses one-dimensional simulation to examine air dynamics for individual cylinders on a cycle-to-cycle basis. The main objective is to provide information such as cylinder air charge, residual fraction and cylinder net mean effective pressure (NMEP) at various firing sequences, which can then be used for air estimator design which in practice uses a limited set of sensor measurements such as mass airflow (MAF) and intake manifold pressure (MAP) to obtain cylinder parameters such as air charge. In this paper we will examine several different sample conditions such as fixed patterns as well as dynamically changing firing sequences which may occur in DSF.

### Model Modifications to Accommodate DSF Operation

Selective firing of engine cylinders typically runs contrary to the normal assumptions of commercially available one-dimensional engine simulation packages and specific modifications and additions need to be made to the model in order for it to produce the cycle-correct results appropriate to dynamic skip fire operation. Here we describe the implementation of a DSF engine simulation in Gamma Technologies' GT-Power environment incorporating these modifications. This model is integrated with a Simulink control strategy model in a co-simulation environment.

### Example Modeled Engine

The engine model discussed here is a GM 6.2L V8, similar to the L94 engine used in a model year 2010 GMC Yukon Denali full size sport-utility vehicle. Specifications of the stock engine are given in Table 1. In the production L94 engine, GM's Active Fuel Management cylinder deactivation system is present which deactivates valves on cylinders 1, 4, 6 and 7 using lost-motion roller hydraulic valve lifters. For implementation of the Tula DSF system, modifications were made to the valvetrain of cylinders 2, 3, 5, and 8 to allow deactivation for all cylinders [1].

Table 1. GM L94 Engine Specifications [10]

Type and Displaced volume	V8, 6162 cm <sup>3</sup>
Bore / Stroke	103.25 mm / 92 mm
Connecting Rod	154.9 mm
Compression ratio	10.4:1
Valvetrain	Overhead valve, two valves per cylinder, dual-equal cam phasing
Deactivation System	Intake and exhaust valve lifters, oil pressure actuated

### Simulation Model Details

Appendix A shows the top level diagram of a detailed GT-Suite engine model. The engine air inlet is represented at the top left, and the flowpath of the intake air is towards the top center of the figure. The intake air enters the intake manifold, shown in the center of the figure. Four cylinders are shown on the left and right sides of the center intake plenum, representing the left and right banks of the engine. After exiting the cylinders, the exhaust system of each bank is modeled as entering an exhaust header, which then flows through a catalyst and exits to ambient.

The engine model consists of eight independent cylinder models, one intake manifold sub-model and two exhaust system sub-models. The sub-models are stored in external subassemblies. There are total of 105 flow elements in intake manifold models and 10 in the exhaust manifold for each bank.

This detailed model was simplified to create a fast running model (FRM). In the FRM, a number of flow elements are lumped together and a coarse discretization grid is used in order to decrease time required for simulation execution. The FRM was used in the following section for cylinder air mass (MAC) and NMEP prediction with varying firing density.

Figure 2 shows the intake and exhaust runner model elements for a representative cylinder. The intake runner is split into two elements, representing the intake runner in the intake manifold and the intake runner in the cylinder head. An orifice between the plenum and the intake runner in the manifold, and another between the manifold and the cylinder head port, are included. The exhaust system for cylinders of each bank is modeled by a single lumped volume. Port dimensions for all elements are typically obtained from measurements of physical engine components.

#### Intake, Cylinder and Exhaust Model

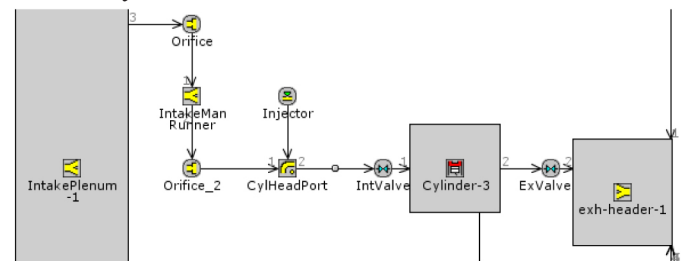


Figure 2. FRM Intake and exhaust runner models. Elements used to determine control of intake and exhaust valves and mass of fuel injected are omitted for clarity

The discretization length for the FRM intake components was set to 30 mm, and that for exhaust components was set to 43.5mm.

#### Method to Deactivate Cylinders

Selective firing controlled by an external Simulink model requires additional elements be introduced in the GT model. Figure 3 shows the elements used to disable the intake valve, exhaust valve, and combustion. The Simulink model representing the engine controller interfaces with the valve lift multiplier blocks connection to the intake and exhaust valves.

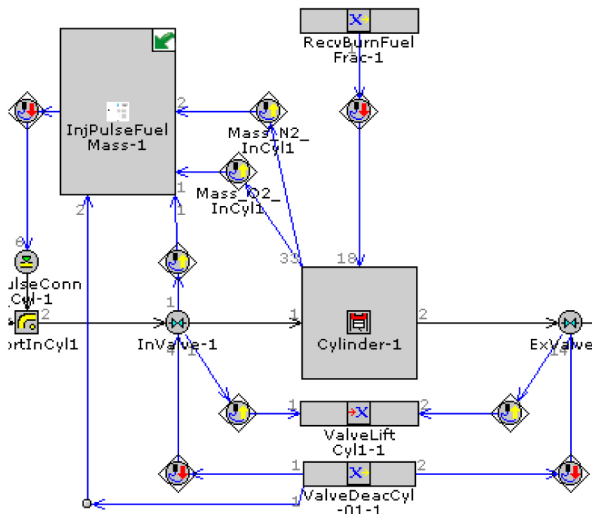


Figure 3. Elements required for cylinder deactivation

### Fuel Injection Control

The fuel injector model container shown in the upper left corner of Figure 3 is expanded in Figure 4. The fuel control determines the air mass and injects the appropriate amount of fuel into the port. In the simulation model for this study, the amount of fuel injected is proportional to the trapped air mass in the cylinder when the intake valve closes. The trapped air mass is calculated based on instantaneous variables internal to the GT simulation (aka “sensed variables”) rather than via air estimation algorithms in the controller model, resulting in near-perfect fueling for every event. This was done in order to avoid the possibility of air estimation errors affecting the simulation results.

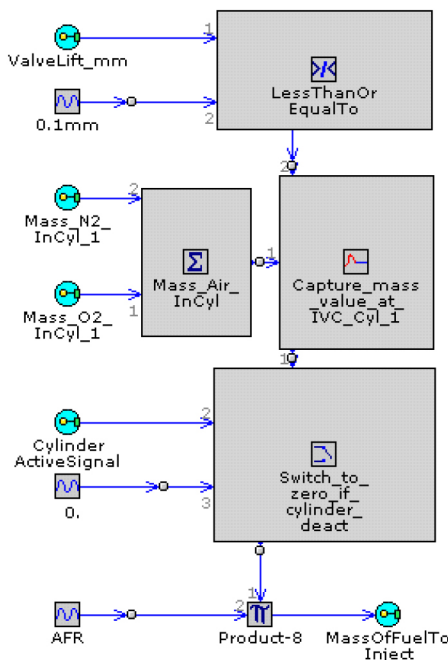


Figure 4. Detail of algorithm used to control mass of fuel injected into the intake port

### Combustion

Combustion parameters were predicted based on a simple Wiebe function, the coefficients of which were derived from experimental data and compiled into lookup tables based on manifold pressure, cam phasing, and engine speed. Heat transfer rates to the cylinder wall were evaluated based on a simple Woschni model. Parameters for the Wiebe function and the Woschni models were based on V8 data and not altered for dynamic skip fire operation.

In the GT framework, combustion parameters are only read at local start of cycle. To accommodate skipping, the combustion object was deactivated for the skipping cycles. Cylinder deactivation was performed by exhaust gas trapping after the exhaust stroke. The exhaust valve is always active after every combustion event and the majority of the cylinder contents are exhausted. When a skip event is desired the intake valve is deactivated, fuel and spark are disabled, and the exhaust valve is deactivated. Upon the command for a fire event the cycle begins with the intake valve being re-activated.

### Validation of Fast Running Simulation Model

#### Engine Operating Conditions

Excluding idle, the fuel-consumption-weighted, average operation of this platform on the U.S. five drive cycles is roughly 1500 RPM. Thus that engine speed was chosen for the following comparisons.

The most fuel-efficient combination of manifold pressure and camshaft phasing, while maintaining good combustion stability, is generally near 90kPa and 40 crank-degrees of camshaft retard. As such, all dynamic skip fire simulation results presented here are for those conditions.

#### Predicted In-Cylinder Pressure

As an example to facilitate understanding of the process used, the cylinder pressure resulting from a firing density of 33% (one fire followed by two skips, also known as a ‘12 stroke’ in some publications) is shown in figures 5, 6, 7, 8, 9. The firing order for this engine is 1-8-7-2-6-5-4-3, if the engine cycle begins with firing cylinder #1, cylinders 1, 3 and 7 are fired in engine cycle #1, followed by cylinders 8, 6, and 2 in engine cycle #2 and then cylinder 4 and 5 in engine cycle #3 to complete the sequence, as illustrated in figure 5. In this condition, each cylinder fires once and is then deactivated for two engine cycles.

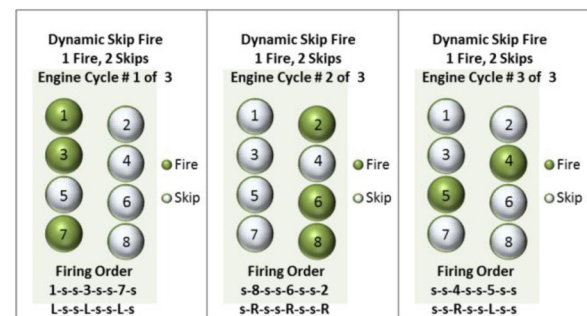


Figure 5. An example of a firing sequence that fires one cylinder followed by two skipped cylinders. The pattern repeats after three engine cycles for an 8 cylinder engine

Figure 6 shows simulated and experimentally measured cylinder pressures as a function of crank angle. On a linear scale the simulation is seen to track experiment closely. The simulation correctly disables the intake valve before cycle 2, and re-enables it midway through cycle 3.

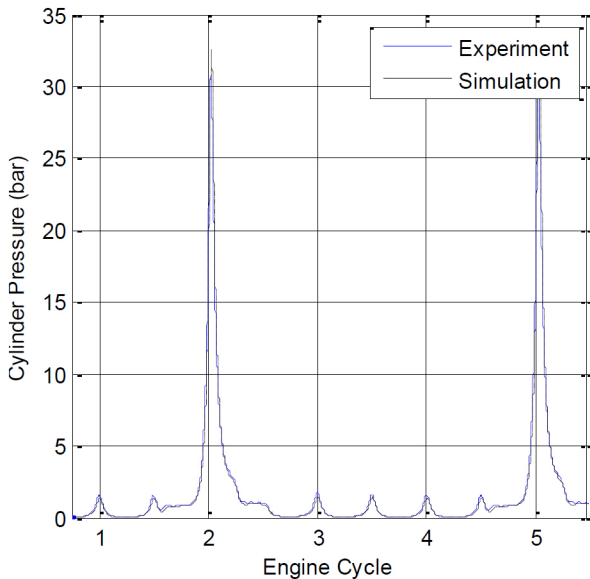


Figure 6. Cylinder pressure vs. crank angle for 3 consecutive engine cycles for 33% firing density

Figure 7 shows a p-V diagram for cycle 1, in which an intake event that occurred previously is compressed, fired, and exhausted. As the cylinder will then be deactivated for two cycles, the intake valve is not activated and the cylinder pressure decreases to sub-atmospheric during the piston motion that would correspond with an intake event.

Figure 7 shows good correspondence between simulation and experiment during the compression, combustion, and expansion portion of the thermodynamic cycle. Pressure at TDC of gas exchange is shown to be slightly lower than is measured and that difference continues throughout the remainder of the deactivated intake stroke.

Figure 8 shows the p-V diagram for the first complete skipping cycle, Cycle 2. As is shown the total change in pressure for the four deactivated strokes is quite small. Pressure varies between about 0.08 and 1.8 bar; the higher pressure at TDC is a result of the large residual mass remaining in the cylinder due to the highly retarded cam phase. The cylinder pressure transducer signal to noise ratio causes the apparently large amount of variation at the lowest pressures when viewed on this logarithmic scale.

Figure 9 shows the p-V diagram for the second skipping cycle, Cycle 3. As plotted here the cycle ends with an intake event in preparation for the next cycle, in which the cylinder is fired. Although the simulated cylinder pressure shows some deviation from the experimental measurement during the intake stroke, at BDC the error is small.

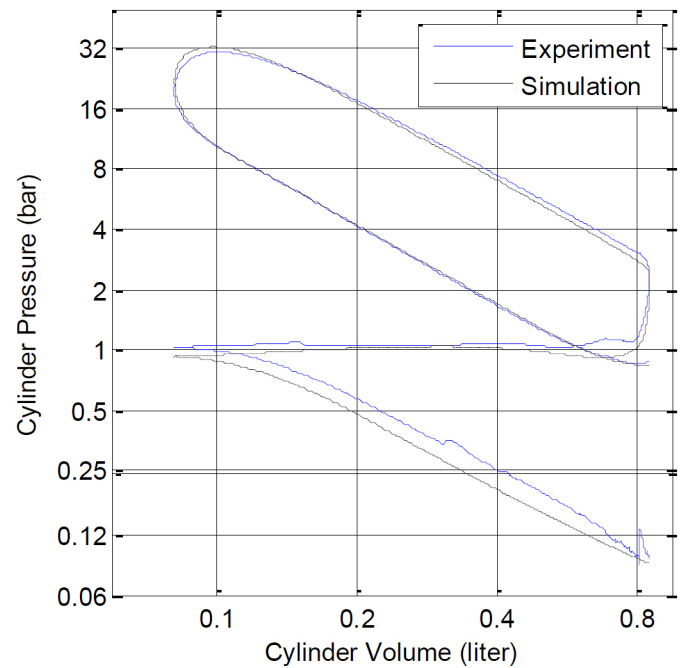


Figure 7. p-V diagram for Cycle 1 firing event

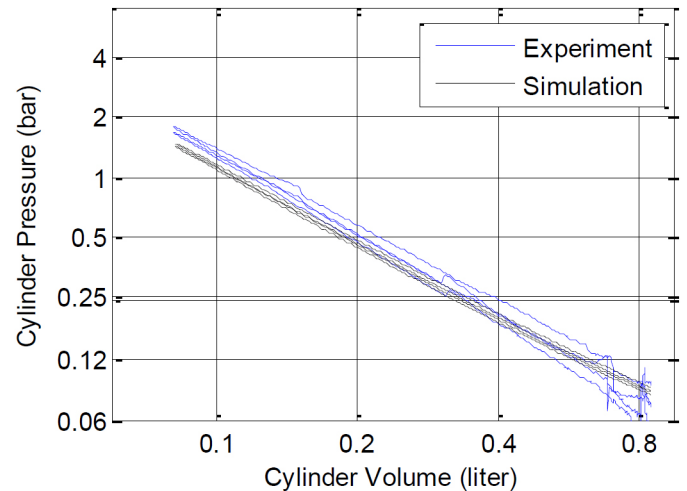


Figure 8. p-V diagram for first skipping event (Cycle 2)

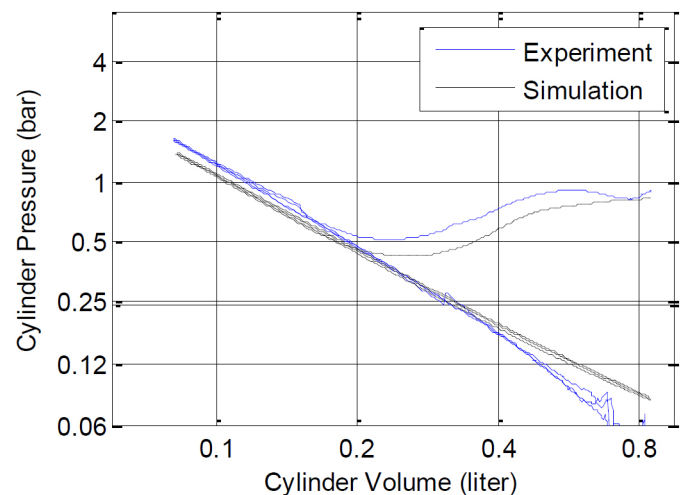


Figure 9. p-V diagram for second skipping event (Cycle 3)

### Cylinder Air Charge Prediction

As the cylinder pressure at BDC before compression is similar between simulation and experiment, we would expect reasonable prediction of air consumption. Figure 10 shows a comparison between simulated and experimentally measured cylinder air charge, expressed as a percent deviation from V8 operation at the same average manifold pressure. When reducing firing density from 100% to 30%, the general trend of a small increase in cylinder air charge is seen both in experimental results and in simulations.

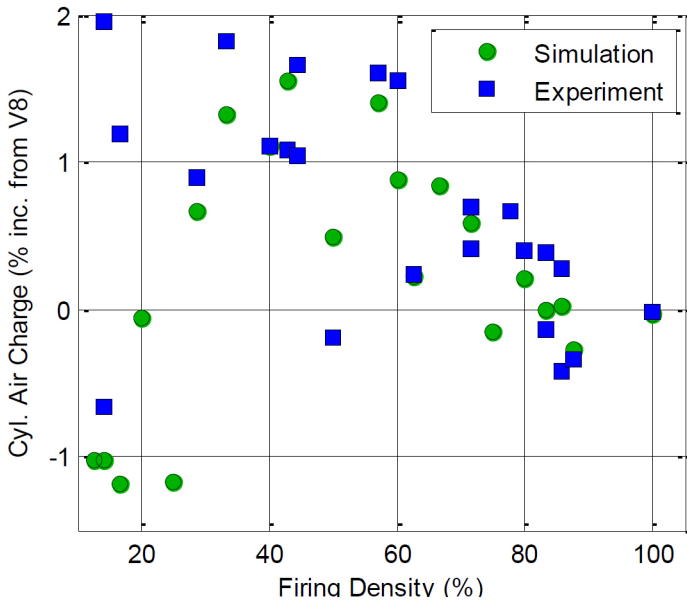


Figure 10. Deviation in mass of trapped air per firing event compared with V8 operation, as a function of firing density

Figure 11 shows the discrepancy between simulation and experiment in air charge. Above 20% firing density, the error is less than 1.1% throughout the conditions tested. Below 20% firing density, the error magnitude increases to a maximum of close to 3%.

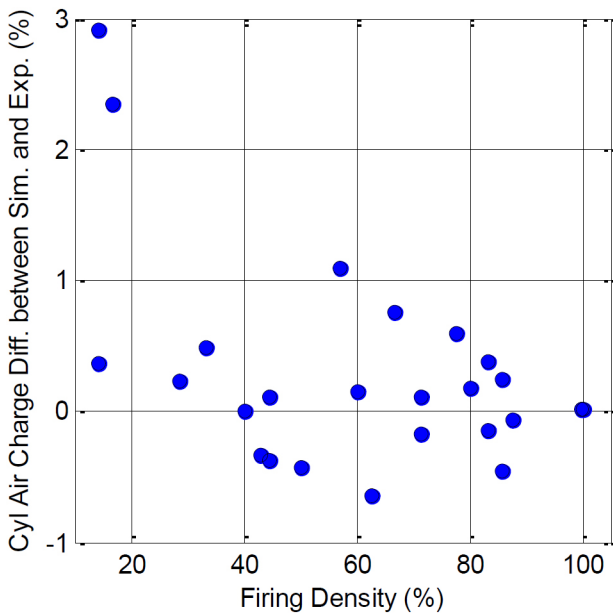


Figure 11. Relative difference in predicted and experimentally measured cylinder air charge, as a function of firing density

### Engine Net Mean Effective Pressure

Figure 12 shows average NMEP for firing cylinders as a function of firing density, for experiment and simulation. Figure 13 shows the difference between simulated and experimental NMEP for the conditions shown, displaying a difference of less than 0.15 bar for all conditions.

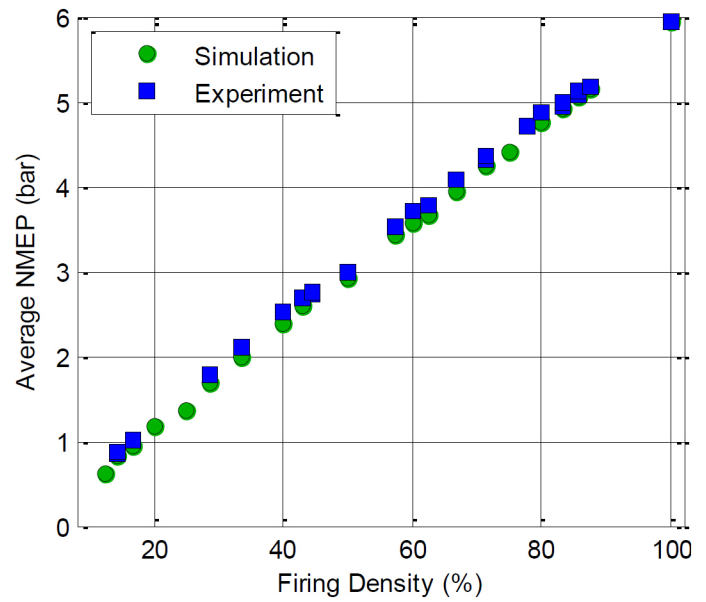


Figure 12. Firing event NMEP as a function of firing density, comparison of simulation and experiment

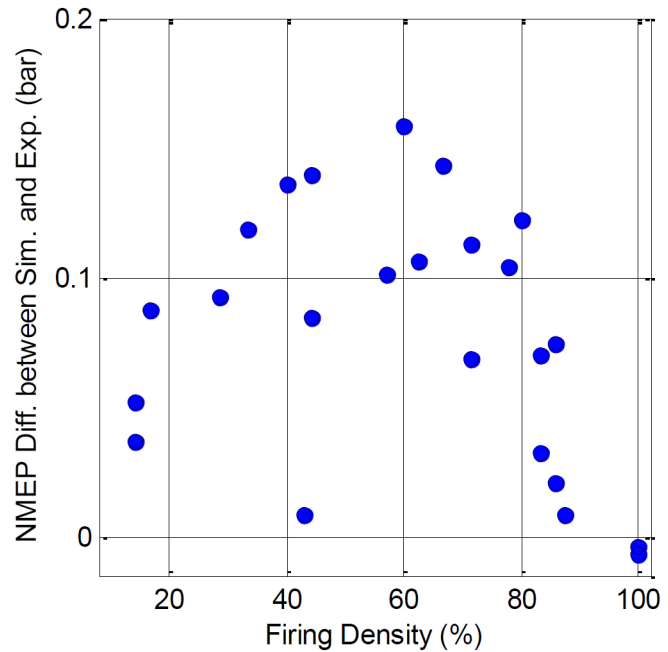


Figure 13. Difference between experimental and simulated firing event NMEP

Error due to the combustion parameters and airflow model parameters being extracted from V8 operational data appears to be minimal. At firing densities less than 100%, the NMEP predicted in simulation is generally slightly less than was realized in the experiment; which is partially due to the error in air prediction and partially due to slight combustion parameter errors.

## Net Specific Fuel Consumption

Figure 14 shows net indicated specific fuel consumption (NSFC) vs. NMEP for simulated and experimental DSF as well as V8 operation. Between 2 and 6 bar, simulation and experimental results are in close agreement. Below 2 bar, the simulated results show some deviation from experimental results. For reference, best fuel-consumption V8 operation is included; at 2 bar, both simulation and experiment indicate a NSFC of 235 g/kW-hr, a 32% improvement over V8 operation.

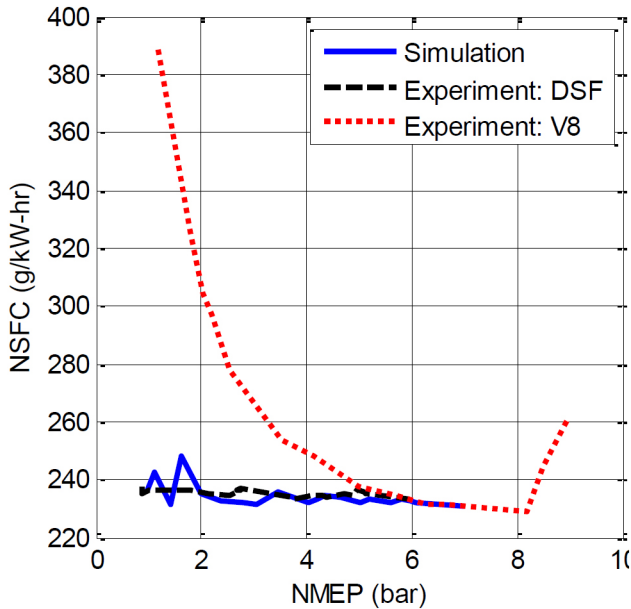


Figure 14. Net indicated specific fuel consumption as a function of NMEP for measured and experimental DSF as well as V8

## Prediction of Cylinder Air Charge and NMEP using Detailed Engine Model

### Air Dynamics for Various Firing Patterns

Dynamic skip fire achieves engine torque control via density of cylinder firings. This flexibility also means phenomena relevant to skip fire operation must be included in engine control schemes. Under given average manifold conditions, different firing sequences with the same firing density may yield different per-cylinder air consumption and torque characteristics. In order to more accurately capture the intake and exhaust gas dynamics, in this section the detailed GT engine model was used.

For the results in this section the model was configured to operate at a constant inlet air flow rate using a closed loop MAF controller targeting 20 g/s average air flow. The cam retard was fixed at zero and engine speed at 1500 rpm. The transient GT simulation was allowed to settle to steady state and MAC and NMEP for each cylinder were tabulated for the last cycle, or set of cycles defining a complete firing sequence. The firing sequences shown in the tables represent the fire or skip state for each cylinder in each cycle.

#### Case 1

Table 2 shows that in Case 1, where all cylinders fire, the MAC and NMEP are very nearly uniform across all cylinders, as is to be expected.

Table 2. Cylinder Air Charge and NMEP for Case 1 (V8 operation)

Engine Cycle	Cylinder							
	1	8	7	2	6	5	4	3
Cycle 1	1	1	1	1	1	1	1	1
MAC (mg)								
Cycle 1	201	198	199	200	202	203	193	204
NMEP (bar) , NSFC=319(g/kWh)								
Cycle 1	2.0	2.0	2.0	2.0	2.0	2.1	1.9	2.1

#### Case 2

Table 3 shows the simulation outcome for Case 2, a 50% firing density operation using a fixed cylinder sequence in which only cylinders 1, 4, 6 and 7 fire while the other cylinders skip throughout the simulation. This type of fixed cylinder mode is commonly used in conventional cylinder deactivation applications.

For the same total engine air flow, 50% firing density operation has correspondingly doubled air charge, on average. Higher air charge indicates higher manifold pressure which reduces pumping losses. This reduction in pumping loss is reflected in the 18.5% reduction in NSFC.

The differences in MAC and NMEP between firing cylinders are larger than in V8 mode. These differences are primarily due to breathing differences caused by intake and/or exhaust manifold pressure dynamics. This particular sequence has two firings on the left cylinder bank followed by two firings on the right bank of cylinders.

Table 3. Cylinder Air Charge and NMEP for Case 2, a 50% Firing Density Fixed Cylinder Operation

Engine Cycle	Cylinder							
	1	8	7	2	6	5	4	3
Cycle 1	1	0	1	0	1	0	1	0
MAC (mg)								
Cycle 1	403	0	406	0	398	0	393	0
NMEP (bar) , NSFC=241 (g/kWh)								
Cycle 1	5.4	-0.1	5.4	0.0	5.3	0.0	5.3	0.0

#### Case 3

Case 3, also with 50% firing density, alternates between firing cylinders 1, 4, 6 and 7 in cycle 1 then firing cylinders 2, 3, 5 and 8 in the subsequent cycle. Table 4 shows that the differences between

firing cylinders in a rotating-cylinder sequence are larger than with the fixed-cylinder sequence of case 2. The nonzero NMEP for skipped cylinders is the result of window definition for the NMEP calculation starting at BDC before compression.

Table 4. Cylinder Air Charge and NMEP for Case 3, a 50% Firing Density Rotating Cylinder Operation

Engine Cycle	Cylinder							
	1	8	7	2	6	5	4	3
Cycle 1	1	0	1	0	1	0	1	0
Cycle 2	0	1	0	1	0	1	0	1
MAC (mg)								
Cycle 1	397	0	400	0	395	0	391	0
Cycle 2	0	407	0	404	0	409	0	397
NMEP (bar) , NSFC=239(g/kWh)								
Cycle 1	5.1	0.3	5.1	0.3	5.1	0.3	5.0	0.3
Cycle 2	0.3	5.2	0.3	5.2	0.3	5.3	0.3	5.1

**Case 4**

Case 4 is a 33% firing density sequence with regularly-spaced firings. The cylinder air charges are higher than in the 50% firing density operation since the engine air flow is regulated to the same value as before. Table 5 shows that in this mode the differences between cylinders are negligible for both air charge and NMEP.

Table 5. Cylinder Air Charge and NMEP for Case 4, a 33% Density Firing Sequence with Regularly-Spaced Firings

Engine Cycle	Cylinder							
	1	8	7	2	6	5	4	3
Cycle 1	1	0	0	1	0	0	1	0
Cycle 2	0	1	0	0	1	0	0	1
Cycle 3	0	0	1	0	0	1	0	0
MAC (mg)								
Cycle 1	603	0	0	596	0	0	596	0
Cycle 2	0	600	0	0	600	0	0	600
Cycle 3	0	0	603	0	0	602	0	0
NMEP (bar) , NSFC=232 (g/kWh)								
Cycle 1	7.8	0.6	0.0	7.7	0.6	0.0	7.7	0.6
Cycle 2	0.0	7.7	0.6	0.0	7.7	0.6	0.0	7.7
Cycle 3	0.6	0.0	7.8	0.6	0.0	7.7	0.6	0.0

**Case 5**

Table 6 presents results for Case 5, a 33% firing density sequence with irregularly-spaced firings. The sequence repeats every 9 cycles. The cylinder to cylinder differences are significantly larger than in the 33% firing sequence with regularly-spaced firings.

Table 6. Cylinder Air Charge and NMEP for Case 5, a 33% Density Firing Sequence with Irregularly-Spaced Firings

Engine Cycle	Cylinder							
	1	8	7	2	6	5	4	3
Cycle 1	1	0	0	1	0	1	0	0
Cycle 2	0	1	0	0	1	0	1	0
Cycle 3	0	0	1	0	0	0	0	1
Cycle 4	0	1	0	0	1	0	1	0
Cycle 5	0	0	1	0	0	1	0	1
Cycle 6	1	0	0	1	0	0	0	0
Cycle 7	0	1	0	0	1	0	1	0
Cycle 8	0	0	1	0	0	0	0	1
Cycle 9	1	0	0	1	0	1	0	0
MAC (mg)								
Cycle 1	588	0	0	583	0	577	0	0
Cycle 2	0	604	0	0	600	0	589	0
Cycle 3	0	0	607	0	0	0	0	619
Cycle 4	0	610	0	0	605	0	594	0
Cycle 5	0	0	614	0	0	612	0	581
Cycle 6	581	0	0	579	0	0	0	0
Cycle 7	0	615	0	0	609	0	598	0
Cycle 8	0	0	616	0	0	0	0	608
Cycle 9	611	0	0	606	0	595	0	0
NMEP (bar) , NSFC=223 (g/kWh)								
Cycle 1	7.9	0.6	0.0	7.8	0.6	7.7	0.6	0.0
Cycle 2	0.0	8.2	0.6	0.0	8.1	0.0	7.9	0.6
Cycle 3	0.0	0.6	8.2	0.0	0.6	0.0	0.6	8.1
Cycle 4	0.0	8.1	0.6	0.0	8.0	0.6	7.9	0.5
Cycle 5	0.6	0.0	8.2	0.6	0.0	7.9	0.0	7.8
Cycle 6	7.8	0.6	0.0	7.8	0.6	0.0	0.6	0.0
Cycle 7	0.0	8.2	0.6	0.0	8.1	0.0	8.0	0.6
Cycle 8	0.6	0.0	8.2	0.6	0.0	0.6	0.0	7.9
Cycle 9	8.4	0.0	0.0	8.4	0.0	8.6	0.0	0.0

## Summary of NMEP for All Cases and Comparison to Experimental Results

A summary of NMEP for each of the five cases presented previously are shown in Figure 15 and Figure 16. Figure 15 shows the average NMEP, including skipped cycles, and Figure 16 shows the average of only skipped cycles.

Figure 15 shows that the average NMEP error is 0.016 bar. The maximum error, 0.06 bar, was for case 2, the fixed 50% firing fraction pattern. It is expected that this accuracy is adequate for most uses of engine torque.

Figure 16 shows that the average firing NMEP, which can be used for vibrational study, shows very good correspondence. The maximum discrepancy is 0.12 bar, and average error is 0.032 bar.

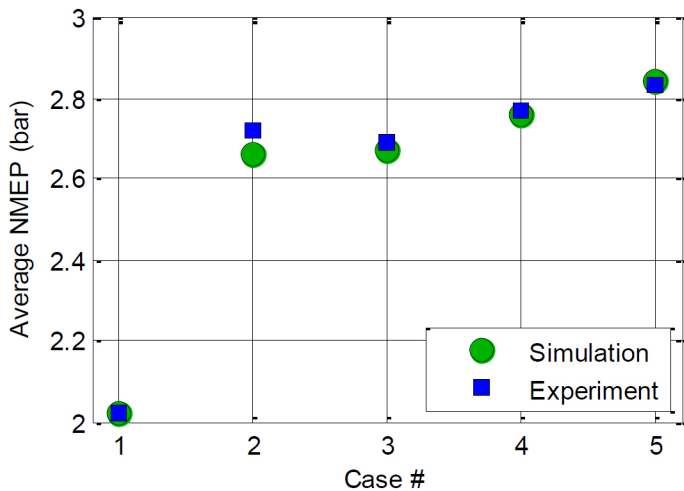


Figure 15. Average NMEP including skipped cycles for each case, simulation and experiment

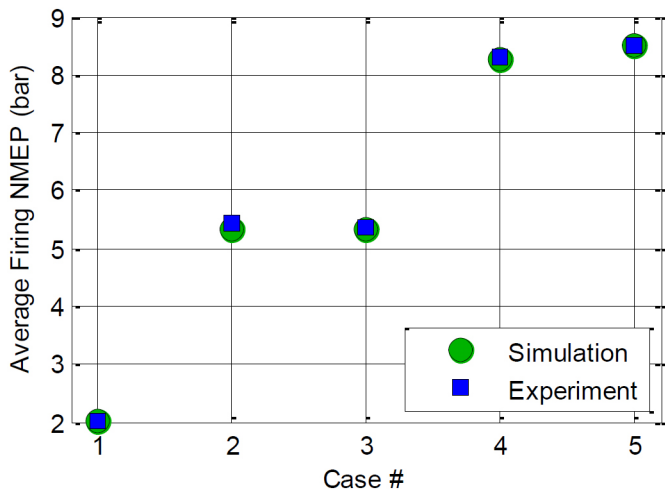


Figure 16. Average firing-only NMEP, simulation and experiment

In practice, Dynamic Skip Fire may use arbitrary firing sequences to match the torque request while also maintaining best fuel conversion efficiency. The results in the section demonstrate that a properly configured engine model can provide sufficiently accurate information regarding the variation of cylinder quantities from firing to firing that would be difficult to measure experimentally. This information can then be used for estimation, control and calibration design.

## Air Charge Compensation

As an example of how the model output could be incorporated in a control scheme, the results for firing by firing air charge are incorporated in an skip compensation scheme for air estimation, as part of a fueling control algorithm.

A typical element in control schemes for all-cylinder firing engines is considering each cylinder to be operating the same, enabling the use of averaged quantities which are the usual output of steady-state dynamometer engine mapping. The results of the preceding section indicate that even in steady state operation the conditions for each cylinder firing may vary depending on the firing sequence. To characterize the dependence of the air charge on relative position of each firing event in the firing sequence, the following parameters to describe the firing history for each firing event can be proposed:

- **Cylinder Skips:** The number of skips preceding each firing for each cylinder in its own firing history. It can be seen as the columns in the firing sequence tables above.
- **Order Skip:** The number of skips preceding each cylinder firing in the firing order. It can be seen as the rows in the firing sequence tables above.

Firing events can be categorized by these two parameters. Using the irregularly spaced firings in the sequence in Table 6 as an example, we can obtain the sequence characterization array in Table 7. In this table the first number in the parentheses represents cylinder skips and the second one represents order skips. Only the firing events are counted since MAC need not be estimated for non-firing events. The non-firing events are shown as zeros.

Table 7. Skip-Fire Characterization Array for the Irregularly Spaced 33% Firing Density Example

	Skip Array (Cylinder Skips, Order Skips)							
Cycle 1	(0,2)	(0,0)	(0,0)	(0,2)	(0,0)	(0,1)	(0,0)	(0,0)
Cycle 2	(0,0)	(0,3)	(3,0)	(3,0)	(0,2)	(3,0)	(0,1)	(0,0)
Cycle 3	(0,0)	(3,0)	(0,3)	(0,0)	(0,0)	(0,0)	(0,0)	(3,4)
Cycle 4	(0,0)	(0,1)	(1,0)	(1,0)	(0,2)	(1,0)	(0,1)	(0,0)
Cycle 5	(0,0)	(1,0)	(0,3)	(0,0)	(3,0)	(0,2)	(0,0)	(1,1)
Cycle 6	(4,0)	(0,0)	(0,0)	(0,2)	(0,0)	(0,0)	(4,0)	(0,0)
Cycle 7	(0,0)	(0,5)	(2,0)	(2,0)	(0,2)	(2,0)	(0,1)	(0,0)
Cycle 8	(0,0)	(2,0)	(0,3)	(0,0)	(0,0)	(0,0)	(0,0)	(2,4)
Cycle 9	(2,0)	(0,0)	(0,0)	(0,2)	(3,0)	(0,1)	(2,0)	(0,0)

Using the skip characterization array, a compensation scheme can be designed to modify the averaged quantity typically output from a MAC estimator, so that it properly describes intake events based on fire-skip history. An example of compensation values based on 33% firing density data above is shown in Table 8. The row entry is cylinder skips while column entry is order skips. The values in each cell are calculated by correlation analysis of the individual MAC with specific firing history to the average MAC. The cell is left blank if there is no data for that particular combination of the two characterization parameters. For example, the cell with cylinder skip of 0 and order skip of 3, all samples that have skip mode of (0,3) are considered in an ensemble average. This average is then divided by

average MAC obtained using the MAF value. With skip compensation, MAF-derived engine mean MAC can be corrected to include individual cylinder firing history as well as cylinder-to-cylinder interaction.

Table 8. Skip Compensation example based on an Irregularly Spaced 33% Firing Density Example

		Order Skips					
		0	1	2	3	4	5
Cylinder Skips	0	1.000	0.987	0.992	1.018		1.027
	1		0.970				
	2	1.004				1.001	
	3					1.023	
	4	0.989					

These are sample results and the model can be used to predict other quantities which are difficult to measure such as charge temperature and residual fraction, which could then similarly be used, for example, for systematic model-based ignition timing control design.

## Summary

Construction and execution of a simulation model of dynamic skip fire engine operation was conducted. In the one-dimensional simulation, a number of elements needed to be added and modified to properly account for the skip-fire operation.

From the detailed model a fast running model was created. The model was adjusted to match experimentally measured V8 performance data. Without modification for DSF operation the model was able to predict airflow within 3% of experiment at all firing densities tested, and within 1.1% above a 20% firing density. NMEP was predicted to within 0.16 bar for all conditions tested. NSFC showed good agreement between simulation and experiment between 2 and 7 bar NMEP; improvements of 32% were shown over V8 operation.

The detailed model was used for cycle-to-cycle cylinder air charge and NMEP prediction for skip fire operation. Average NMEP was compared to experiment. A study was presented that showed examples of the dependence of air charge and NMEP on skip fire sequence.

Finally, a method of compensation development using the model was presented which characterized each firing event by skip history, both of the particular cylinder as well as previous cylinders in the firing order. An example skip compensation table was presented showing how cylinder breathing differences can be compensated in an air estimation scheme.

## References

1. Wilcutts, M., Switkes, J., Shost, M., and Tripathi, A., "Design and Benefits of Dynamic Skip Fire Strategies for Cylinder Deactivated Engines," *SAE Int. J. Engines* 6(1):278-288, 2013, doi:10.4271/2013-01-0359.

2. Stabinsky, M., Albertson, W., Tuttle, J., Kehr, D. et al., "Active Fuel Management™ Technology: Hardware Development on a 2007 GM 3.9L V-6 OHV SI Engine," SAE Technical Paper 2007-01-1292, 2007, doi:10.4271/2007-01-1292.
3. Falkowski, A., McElwee, M., and Bonne, M., "Design and Development of the DaimlerChrysler 5.7L HEMI® Engine Multi-Displacement Cylinder Deactivation System," SAE Technical Paper 2004-01-2106, 2004, doi:10.4271/2004-01-2106.
4. Fujiwara, M., Kumagai, K., Segawa, M., Sato, R. et al., "Development of a 6-Cylinder Gasoline Engine with New Variable Cylinder Management Technology," SAE Technical Paper 2008-01-0610, 2008, doi:10.4271/2008-01-0610.
5. Förster, H.J., Lübbling B.E., Letsche U., "Process and Apparatus for Intermittent Control of a Cyclically Operating Internal Combustion Engine", U.S. Pat. No. 4509488, 1982.
6. Serrano, J., Routledge, G., Lo, N., Shost, M. et al., "Methods of Evaluating and Mitigating NVH when Operating an Engine in Dynamic Skip Fire," *SAE Int. J. Engines* 7(3):1489-1501, 2014, doi:10.4271/2014-01-1675.
7. Schechter, M. and Levin, M., "Camless Engine," SAE Technical Paper 960581, 1996, doi:10.4271/960581.
8. Cullen M. J., Sumilla G., Christian J. Goralski T, and L. Ford Global Technologies, "Engine system and fuel vapor purging system with cylinder deactivation," Feb. 2006. U.S. Pat.7073494B2
9. Michelini J. and Glugla C., "Control system design for steady state operation and mode switching of an engine with cylinder deactivation," presented at the American Control Conference, 2003. Proceedings of the 2003, 2003, vol. 4, pp. 3125-3129.
10. <http://media.gm.com/media/us/en/gmc/vehicles/yukon/2010/tab1.html>

## Contact Information

The authors can be reached at

[ricky@tulatech.com](mailto:ricky@tulatech.com) or

[matthew@tulatech.com](mailto:matthew@tulatech.com)

## Acknowledgments

The authors would like thank Brandon Most, Matthew Herndon, and Casey Horner for their assistance in test data presented in this paper.

## Definitions/Abbreviations

**BDC** - Bottom dead center

**MAC** - Cylinder mass air charge

**MAF** - Mass air flow

**MAP** - Intake manifold absolute pressure

**NMEP** - Net indicated mean effective pressure

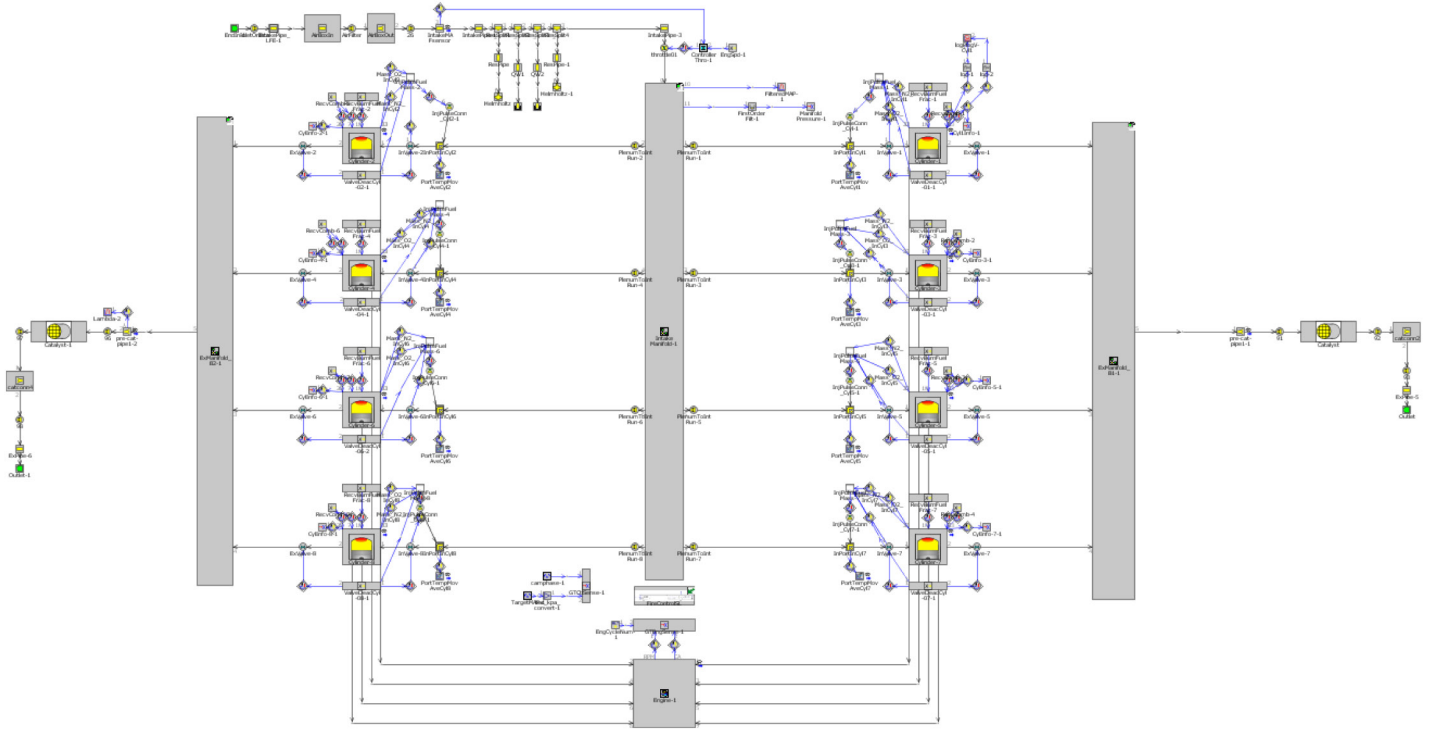
**NSFC** - Net indicated specific fuel consumption

**TDC** - Top dead center

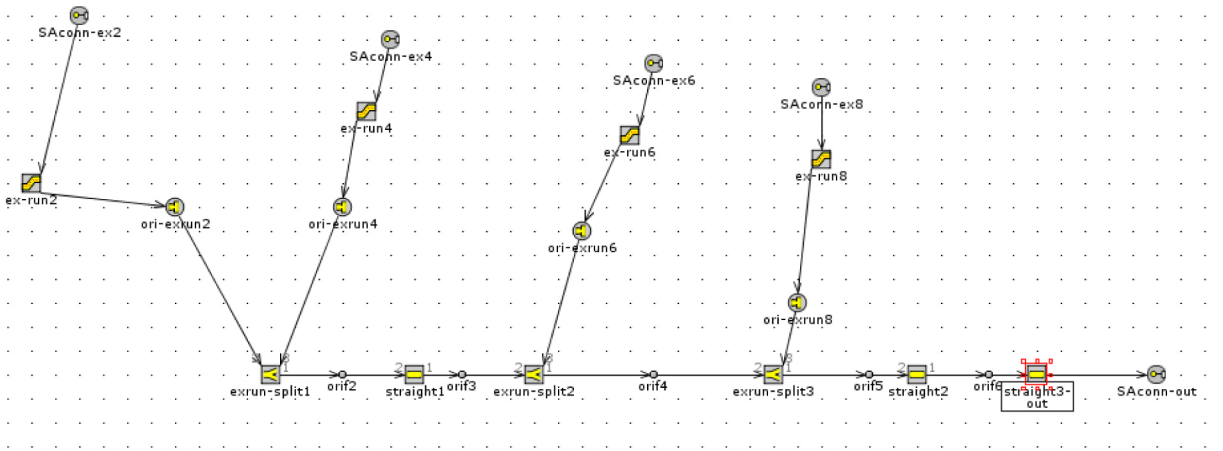
# APPENDIX

## GT-Suite Model Structure

Main engine:



Exhaust manifold (single bank, in subassembly):



The Engineering Meetings Board has approved this paper for publication. It has successfully completed SAE's peer review process under the supervision of the session organizer. The process requires a minimum of three (3) reviews by industry experts.

All rights reserved. No part of this publication may be reproduced, stored in a retrieval system, or transmitted, in any form or by any means, electronic, mechanical, photocopying, recording, or otherwise, without the prior written permission of SAE International.

Positions and opinions advanced in this paper are those of the author(s) and not necessarily those of SAE International. The author is solely responsible for the content of the paper.

ISSN 0148-7191

<http://papers.sae.org/2015-01-1717>